A&A 554, A24 (2013)
DOI: 10.1051/0004-6361/201321052

Astronomy & Astrophysics

Infrared transitions and oscillator strengths of Ca and Mg⋆

S. Civiš[1], M. Ferus[1], V. E. Chernov[1,2], and E. M. Zanozina[1,3]

[1] J. Heyrovský Institute of Physical Chemistry, Academy of Sciences of the Czech Republic, Dolejškova 3, 18223 Prague 8, Czech Republic
e-mail: civis@jh-inst.cas.cz
[2] Voronezh State University, 394693 Voronezh, Russia
e-mail: chernov@niif.vsu.ru
[3] State Research Center of Russian Federation Troitsk Institute of Innovation and Fusion Research, 142190 Troitsk, Moscow Region, Russia

Received 7 January 2013 / Accepted 24 March 2013

ABSTRACT

Aims. While solar spectra contain a lot of Ca I and Mg I infrared (IR) lines, no laboratory-measured spectra of these atoms have been reported for wavenumbers below 2000 cm^{-1}. This study reports Ca I spectra in the 1300–4500 cm^{-1} range and Mg I spectra in the 1300–4500 cm^{-1} range.
Methods. We performed a time-resolved Fourier transform infrared spectroscopy study of a plasma created by the laser ablation of MgF_2 and CaF_2 targets in a vacuum. The oscillator strengths (f-values) were calculated using quantum defect theory (QDT), which shows good agreement with the available experimental and theoretical results.
Results. We report several Ca I and Mg I IR lines that have not been measured previously in laboratory. The recorded spectra allow the excitation energies of some Ca I and Mg I states with high orbital momentum ($l = 4, 5$) to be determined. We also provide a long list of QDT-calculated f-values for Ca I and Mg I in the range of 800–9000 cm^{-1}.

Key words. atomic data – methods: laboratory – techniques: spectroscopic

1. Introduction

Calcium and magnesium are important chemical elements for studying the history of α-process nucleosynthesis. Both these elements are observed relatively easily in the spectra of stars, even in metal-poor star atmospheres, and their overabundance in extremely metal-poor stars is one of the fundamental parameters of the chemical evolution models for our Galaxy (Spite et al. 2012). The abundance of Ca and Mg is sensitive to deviations from local thermodynamic equilibrium (LTE; Zhao & Gehren 2000; Mashonkina et al. 2007; Andrievsky et al. 2010; Spite et al. 2012). Non-LTE corrections to Mg abundance are especially important since magnesium could serve as a better tracer of the chemical evolution of the Galaxy than iron (Andrievsky et al. 2010).

For the stars other than Sun, the non-LTE effects are predominantly studied on the strongest Mg I and Ca I lines in the visible region (Mishenina et al. 2004; Mashonkina et al. 2007). These effects correspond to the radiative transitions from low-excited atomic states. However, including high-excited (Rydberg) atomic states into the atomic models encounters several difficulties (Zhao et al. 1998) that are inherent to the infrared (IR) region.

Although the great advantages of Fourier transform (FT) infrared spectroscopy, such as its constant high resolution and energy throughput, have made the IR spectral region more accessible for high-resolution spectral measurements (Nilsson 2009). The powerful capacities of IR astronomy cannot be fully utilized without detailed spectroscopic information on atomic line features (in particular, wavelengths, and oscillator strengths) in the IR region (Biémont 1994; Johansson 2005; Pickering et al. 2011, see Civiš et al. 2012b, for more references on space- and ground-based IR astronomy). The IR spectrum of the most studied object, the Sun, has been recorded from the ground (Wallace et al. 1996) and from satellite-borne FT spectrometers: ATMOS (Farmer et al. 1989) and ACE FTS (Hase et al. 2010).

In the near-IR domain, lines, most widely used for diagnostic calcium, belong to a well-known triplet (849.81, 854.21, and 866.21 nm), which is due to transition between low-excited $3d$ and $4p$ states of singly ionized Ca II, while the IR lines of neutral Ca I are not so prominent. Three IR solar Mg I lines were observed without identification by ground-based (811.575 and 818.058 cm^{-1}) and balloon-borne (1356.182 cm^{-1}) FT interferometer measurements (Murcray et al. 1981).The strong diagnostic potential of the 12.22 and 12.33 micron Mg I lines was demonstrated by Brault & Noyes (1983). The high Zeeman sensitivity of IR lines (as compared to the visible) permitted them to estimate magnetic field strength in solar low chromosphere. Chang & Schoenfeld (1991) estimated the electric field strength in the Sun using the Stark shift of the above IR Mg I lines. The formation scenario of these line profiles in atmospheres of the Sun (Chang et al. 1991) and K giants (Sundqvist et al. 2008) is substantially explained by non-LTE effects. Using Rydberg formula with a core-polarization correction (Edlén's polarization formula), Chang & Noyes (1983) identified these and some other

⋆ Tables 5 and 6 are only available at the CDS via anonymous ftp to cdsarc.u-strasbg.fr (130.79.128.5) or via http://cdsarc.u-strasbg.fr/viz-bin/qcat?J/A+A/554/A24

Mg I lines in the spectra reported by Murcray et al. (1981) and by Brault & Noyes (1983) as due to transitions between 3*s nl* states of Mg I with high orbital angular momenta $l > 3$ (Chang 1987). Some other solar Mg I lines observed from Kitt-Peak National Solar Laboratory and Spacelab 3 ATMOS experiment in the 800–900 cm^{-1} and 1100–1200 cm^{-1} ranges were studied by Glenar et al. (1988).

Except for the most prominent features, atomic spectra are virtually unchartered territory for wavelengths in the near-IR region and longer; therefore, high-precision IR wavelength calibration requires continued laboratory analysis (Wahlgren et al. 2012).

In past decades only two measurements of Mg I have been reported in IR region. Using a hollow-cathode discharge technique, Biémont & Brault (1986) measured IR spectrum from 1800 to 9000 cm^{-1}. Their Fourier transform spectrometer (FTS) measurements gave the first laboratory observation of 3s *n*g ^{1,3}G terms of Mg I with principal quantum number $n \leq 8$. In total, Biémont & Brault (1986) reported 116 Mg I lines with a proclaimed uncertainty not greater than 10^{-3} cm^{-1}. Lemoine et al. (1990) measured 23 Mg I lines between 740 and 1126 cm^{-1} with a precision of 0.0002 cm^{-1} using a diode-laser spectrometer. Their measurements of high-l transitions $7l$–$9l'$ with $l = 5, 6, 7$ and $l' = 6, 7, 8$ have corrected the correspondent line wavenumbers observed in the solar spectrum (Brault & Noyes 1983) and calculated by Edlén's formula (Chang 1987).

The laboratory IR spectrum of Ca I was partly ($\nu > 4414$ cm^{-1}, i.e. $\lambda < 2265$ nm) recorded in a hollow cathode emission measurement by Risberg (1968). Since that time the only available laboratory study of Ca I IR spectrum has been done by Chang et al. (2000), who measured high-current hollow cathode spectra of calcium from 2000 to 9000 cm^{-1}, using the FTS at the Kitt Peak National Solar Observatory at a resolution of 0.01 cm^{-1}.

The aim of the present study is to observe IR lines in the 1300–2000 cm^{-1} domain where no laboratory Ca I or Mg I spectra have been recorded previously. We report first laboratory observational evidence for some high-l terms of these atoms and provide calculated f-values for the transitions between high-l states. This work continues the series of Fourier transform infrared spectroscopy (FTIR) spectroscopy studies of the IR spectra of metal atoms (Civiš et al. 2012b,c,a).

2. Methods

The IR emission spectrum of Mg I and Ca I was measured using high-resolution FTIR spectroscopy of the plasma formed by the laser ablation of CaF_2 and MgF_2 target. The sample surface was irradiated by a high-repetition-rate, pulsed, nanosecond ArF laser ($\lambda = 193$ nm, laser pulse width 12 ns, frequency 1.0 kHz, output energy 15 mJ) in a vacuum (10^{-2} Torr). The emission from the plasma was focused into the spectrometer by a ZnSe (127 mm) lens for the spectral range below 1600 cm^{-1} and by a CaF_2 (100 mm) lens for the range above 1600 cm^{-1}. The spectra were measured in the different spectral regions with two different detectors. In the 1300–1600 cm^{-1} range a HgCdTe detector was used, while above 1600 cm^{-1} we applied an InSb detector. Generally, the sensitivity of both detectors is different. In our measurement we also applied the narrow interference filters (with specific absorption profiles) to cut the strong laser emission. For that reason the absolute spectral intensity scale cannot be estimated, and we can only get the relative intensities of the emission lines inside a corresponding interference filter window.

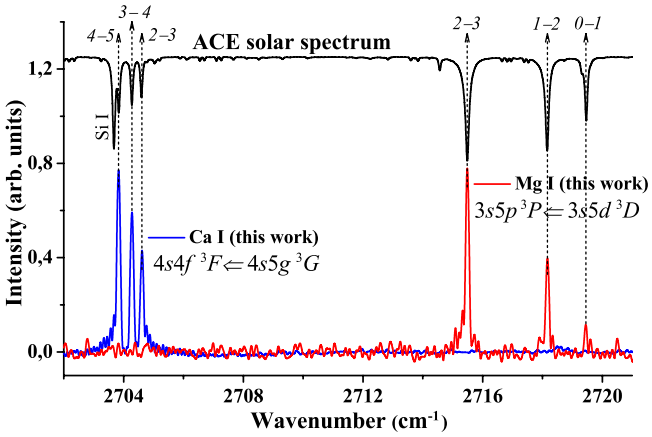

Fig. 1. A part of Mg I and Ca I emission spectra versus the ACE solar spectra (Hase et al. 2010).

Several kinds of noise – electronic noise (PC, cables, connectors, detectors), thermal noise (sample is heated by numerous high-energy laser shots), and mechanical noise (vibrations of the sample and spectrometer are caused by mechanical pumps) – have a strong influence on detection limits but not on the accuracy of the line position. The main source of the obtained wavenumber's error is the statistical errors due to fitting the measured data arrays to a Lorentzian line profile.

For the measurements we used a Bruker 120 FTIR spectrometer, which has a maximum unapodized resolution about 0.003 cm^{-1}. The absolute wavenumber scale is linear and is defined by the internal control HeNe laser, whose frequency is normally stabilized to $\sim 10^{-9}$. In our case, to achieve better signal-to-noise ratio (S/N), we use a multiple-scan scheme, so that our measurement are performed at the maximum resolution about 0.017 cm^{-1}. Therefore the error due to instabilities of the internal HeNe laser does not exceed the latter resolution value and additional calibration is not needed. More details on the experimental setup are given in our previous papers (Kawaguchi et al. 2008; Civiš et al. 2010a,b,2011c,a).

The oscillator strengths were calculated using single-channel quantum defect theory (QDT). This is reasonable for a two-electron atom once only the transitions between 3s *nl* states in Mg I and 4s *nl* states in Ca I are considered. The calculations were done assuming *LS* coupling, and the intercombination transitions were neglected. We compared some QDT-calculated oscillator strengths with experimental and theoretical data available in the literature. As in our previous works (Civiš et al. 2010a,b,2011b, 2012b,c), the overall agreement of our QDT calculations with the results available in other sources is quite satisfactory.

For all tables, uncertainties are reported in parentheses immediately following the values. They should be treated as the rightmost significant digits; e.g., 123.4(56) means 123.4 ± 5.6.

3. Results

A part of the recorded spectra are shown in Fig. 1, where the most prominent lines of two multiplets are shown (4s4f ^{3}F-4s5g ^{3}G for Ca I and 3s5p ^{3}P–3s5d ^{3}D for Mg I). The values of the total angular momenta of the lower and upper states are specified above the corresponding lines as for J–J'. The observed lines are shown together with the corresponding Ca I and Mg I in solar spectra recorded by ACE-FTS (Hase et al. 2010).

Table 1. Ca I lines observed in this work.

ν_{ki}, cm^{-1}			Line parameters			Identification
This work	ACE	Chang et al. (2000)	I_{ki} (arb. u.)	S/N	$FWHM$, cm^{-1}	
1374.276(5)	1374.30		8.53×10^3	12.1	0.070(13)	4s5g ^{3}G–4s6h ^{3}H
1374.696(8)	1374.72		5.00×10^3	6.16	0.074(23)	4s5g ^{1}G–4s6h ^{1}H
1426.794(12)	1426.83		1.81×10^3	5.22	0.053(25)	4s5f ^{1}F$_3$–4s6g ^{1}G$_4$
1454.163(15)	1454.18		1.58×10^3	3.57	0.066(44)	4s6p ^{3}P$_2$–4s7s ^{3}S$_1$
1467.915(4)	1467.94		1.24×10^3	3.94	0.053(30)	4s5f$^3F_4$–4s6g^{3}G$_5$
1468.182(16)	1468.19		3.46×10^4	20.0	0.081(9)	4s5f^{3}F$_{2,3}$–4s6g^{3}G$_{3,4}$
2015.695(5)	2015.73		2.16×10^3	10.3	0.072(16)	4s5d ^{3}D$_3$–4s5f ^{3}F$_4$
2018.097(6)	2018.12		1.56×10^3	10.5	0.075(20)	4s5d ^{3}D$_2$–4s5f ^{3}F$_3$
2019.608(5)	2019.62		1.06×10^3	6.57	0.059(22)	4s5d ^{3}D$_1$–4s5f ^{3}F$_2$
2040.600(18)	2040.60		2.19×10^2	3.04	0.045(54)	4s6s ^{3}S$_1$–4s6p ^{3}P$_0$
2044.450(7)	2044.47		1.16×10^3	10.4	0.074(18)	4s6s ^{3}S$_1$–4s6p ^{3}P$_1$
2052.320(4)	2052.35		2.22×10^3	15.6	0.080(12)	4s6s ^{3}S$_1$–4s6p ^{3}P$_2$
2185.628(11)	2186.06		6.73×10^2	5.34	0.078(34)	4s5g–4s7h
2244.032(4)	2244.03		3.20×10^2	3.27	0.080(28)	4s5f ^{1}F$_3$–4s7g ^{1}G$_4$
2285.497(11)			3.06×10^2	4.63	0.063(41)	4s5f ^{3}F–4s7g ^{3}G
2525.683(7)	2525.69		1.94×10^3	7.02	0.097(22)	4s6p ^{3}P$_2$–4s6d ^{3}D$_3$
2530.833(4)	2530.31	2530.8394	1.42×10^4	6.80	0.112(14)	4s6p ^{3}P$_1$–4s6d ^{3}D$_1$
2531.644(8)	2531.74		9.28×10^2	3.48	0.063(36)	4s6p ^{3}P$_1$–4s6d ^{3}D$_2$
2597.630(13)	2597.53		1.19×10^2	3.35	0.030(76)	4s6p ^{1}P$_1$–4s7s ^{1}S$_0$
2703.832(7)	2703.85	2703.849	2.09×10^4	5.49	0.107(22)	4s4f ^{3}F$_4$–4s5g ^{3}G$_5$
2704.276(14)	2704.29	2704.2862	1.92×10^4	4.02	0.123(67)	4s4f ^{3}F$_3$–4s5g ^{3}G$_4$
2704.613(7)	2704.61	2704.6044	1.18×10^4	2.80	0.113(24)	4s4f ^{3}F$_2$–4s5g ^{3}G$_3$
3263.342(10)	3263.35		3.43×10^2	6.42	0.072(32)	4s5d ^{1}D$_2$–4s6f ^{1}F$_3$
3414.338(3)	3414.35		8.15×10^3	28.3	0.130(9)	4s5s^{1}S$_0$–4s5p^{1}P$_1$
4336.523(5)	4336.52	4336.5252	7.14×10^4	16.1	0.096(13)	3d4p ^{1}F$_3$–4s5g ^{1}G$_4$
4380.739(12)	4380.72		2.91×10^4	3.78	0.089(42)	4s4d ^{1}D$_2$–4s6p ^{1}P$_1$
4413.061(21)	4413.11		6.29×10^4	3.13	0.058(49)	4s4d ^{3}D$_3$–4s4f ^{3}F$_3$
4413.554(4)	4413.58		1.24×10^6	11.6	0.110(13)	4s4d ^{3}D$_3$–4s4f ^{3}F$_4$
4418.313(12)	4418.35		6.48×10^4	3.48	0.058(38)	4s4d ^{3}D$_2$–4s4f ^{3}F$_2$
4418.684(4)	4418.69		8.54×10^5	15.9	0.107(12)	4s4d ^{3}D$_2$–4s4f ^{3}F$_3$
4422.013(4)	4422.02		5.54×10^5	11.1	0.108(13)	4s4d ^{3}D$_1$–4s4f ^{3}F$_2$

3.1. Ca lines

In Table 1 we list our observed lines of Ca I with their parameters and identification. The measurements were performed in three spectral ranges: 1300–1600, 2000–4000, and 4000–4500 cm^{-1}. The arbitrary units of intensity are valid only within the same (of the above three) spectral range.

Table 1 also shows a comparison of our results with other measurements, i.e. with laboratory high-current hollow-cathode spectra of calcium using the one-meter FTS at the McMath-Pierce solar telescope operated by the National Solar Observatory at Kitt Peak (Chang et al. 2000) and with a solar spectrum atlas measured from the space-borne ACE-FTS (Hase et al. 2010). The spectral resolutions of these two measurements were 0.01 and 0.005 cm^{-1} respectively. For the majority of the lines, our wavenumbers agree with the other measurements within the specified uncertainties. No laboratory measured Ca I have been previously available below 2530 cm^{-1}. As an example, in Fig. 2 we plot two measured Ca I ablation spectrum lines corresponding to the 5g–6h transitions between the triplet and singlet states. Since the fine splitting is very small for high-l states, no fine structure of these lines is resolved in the present spectrum or in ACE-FTS spectrum, which is also shown in Fig. 2.

In Table 2 we compare some multiplet f-values (i.e., summed over the fine structure components) with calculations by Hansen et al. (1999) used a model-potential method. Although some of our values disagrees with Hansen et al. (1999) significantly, the overall agreement is satisfactory and improves with the increase in the principal quantum numbers n, n', as it should be, given that the higher-excited atomic states are better described by QDT than by the low-excited states.

In Table 5 we present the matrix elements (f- and A-values) for the transition involving the 4snd, 4snf, 4sng, and 4snh states of Ca I in the 800–9000 cm^{-1} range. The Ritz wavenumbers ν

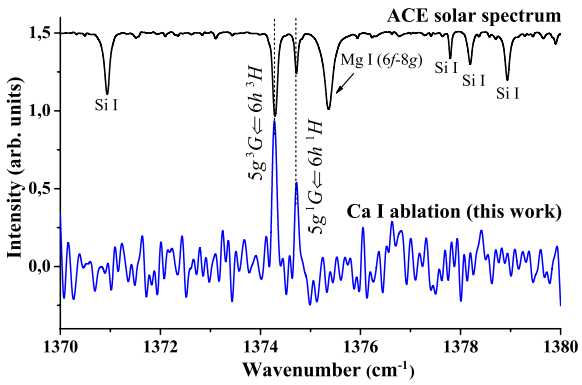

Fig. 2. 5g–6h Ca I lines from the ablation plasma spectrum (this work) and ACE solar spectrum (Hase et al. 2010).

Table 2. Multiplet f-values for several $4s\,nl\,S$–$4s\,n'l'\,P$ transitions in Ca I.

$4s\,ns \leftarrow 4s\,n'p$									
		5p		6p		7p		8p	
		^1S–^1P	^3S–^3P	^1S–^1P	^3S–^3P	^1S–^1P	^3S–^3P	^1S–^1P	^3S–^3P
6s	[1]	–0.4310	–0.7513	0.6041	1.802	0.1127	0.05513	0.03070	0.01133
	[2]	–0.7224	–0.7544	1.130	1.818	0.1891	0.06202	0.05094	0.01428
7s	[1]	–0.0879	–0.07423	–0.3403	–1.307	1.7170	2.268	0.1438	0.07550
	[2]	–0.0762	–0.07714	–0.3702	–1.298	2.064	2.253	0.1388	0.07864
8s	[1]	–0.0328	–0.02463	–0.0704	–9.717	–1.5708	–1.720	2.4519	2.694
	[2]	–0.0274	–0.02621	–0.0728	–9.659	–1.858	–1.703	2.646	2.680
$4s\,np \leftarrow 4s\,n'd$									
		5d		6d		7d			
		^1S–^1P	^3S–^3P	^1S–^1P	^3S–^3P	^1S–^1P	^3S–^3P		
4p	[1]	0.2646	0.1119	0.04527	0.04933		0.02573		
	[2]	0.1167	0.08476	0.04013	0.03890	0.0124	0.02185		
5p	[1]	0.2513	0.3018	0.1352	0.1144		0.06512		
	[2]	0.2262	0.2909	0.1167	0.09789	0.0551	0.04839		
6p	[1]	0.6437	0.2497	0.1172	0.4253		0.1253		
	[2]	1.101	0.2193	0.0962	0.4574	0.0861	0.1399		
7p	[1]	–0.0012	–0.1079	–0.7102	0.2655		0.5198		
	[2]	–0.00037	–0.009354	–0.8375	0.2359	1.799	0.5565		
8p	[1]	–0.0002667	–0.02078	–0.0004333	–0.1427		0.1082		
	[2]	–0.003215	–0.01757	–0.0002868	–0.1339	–1.086	0.09796		
$4s\,nd \leftarrow 4s\,n'f$									
		4f		5fp		6f		7f	
		^1S–^1P	^3S–^3P	^1S–^1P	^3S–^3P	^1S–^1P	^3S–^3P	^1S–^1P	^3S–^3P
5d	[1]	–0.1698	–0.1938	1.094	1.256	0.08856	0.1243	0.01982	0.03303
	[2]	–0.1984	–0.1816	1.347	1.295	0.1246	0.1439	0.03224	0.04196
6d	[1]	–0.00012	-6.0×10^{-5}	–0.2450	–0.3646	1.084	1.335	0.1704	0.1759
	[2]	–0.00352	-6.3×10^{-5}	–0.2571	–0.3616	1.216	1.371	0.2021	0.1897
7d	[1]	–0.00004	-1.3×10^{-10}	–0.02086	–0.001067	–0.06076	–0.4393	0.7998	1.278
	[2]	–0.00032	-2.2×10^{-4}	–0.02938	–0.001719	–0.06599	–0.4604	0.9197	1.358

References. [1] Hansen et al. (1999); [2] This work.

and air wavelengths λ were calculated using the energy level values from the cited references.

3.2. Mg lines

The Mg I lines we observed are presented in Table 3 with their parameters and identification. These spectra were recorded in the following spectral regions: 1200–1600, 1800–3200, 1800–3500, 4100–5000, and 5000–7000 cm^{-1}. As in Table 1, each region has its own scale of arbitrary units for the emission intensity $I_{\rm ki}$. Our measured wavenumbers in Table 3 are compared with experimental wavenumbers listed in NIST Atomic Spectra Database (ASD), which reproduces the data from the laboratory measurement by Biémont & Brault (1986). Table 3 also shows the wavenumbers from ACE solar spectra (Hase et al. 2010).

The majority of our lines appear in the work by Biémont & Brault (1986) except for the transitions from the 6g, 7g, and 7h states. In some cases we see only one line instead of a pair of lines observed by Biémont & Brault (1986). The other components of these multiplets was not resolved due to their low intensity and close wavenumbers (i.e. fine splitting), which can be seen from the transition wavenumbers and probabilities presented in Table 6 below. However, we did observe two lines instead of the one 2291.50 cm^{-1} line observed by Biémont & Brault (1986). Most of our measured line wavenumbers agree either with ACE (Hase et al. 2010) or with Biémont & Brault (1986). We were not able to restore the uncertainty of the wavenumbers from Biémont & Brault (1986), who refer to Brault (1976) where their spectrometer's resolving power of 500 000 is mentioned. One can conclude therefore that in the 2000–7000 cm^{-1} the wavenumber uncertainties of Biémont & Brault (1986) are in the range 0.004–0.014 cm^{-1}.

Table 6 presents f- and A-values for the transition involving the 3snd, 3snf, 3sng, and 3snh states of Mg I in the 800–9000 cm^{-1} range. As in Table 5, the wavenumbers and wavelengths are calculated, see the references cited on the bottom. This Table 6 also contains f-values taken from NIST ASD (Ralchenko et al. 2011) for comparison. The agreement between NIST values and our QDT calculations for Mg I is better than in the case of Ca I; more than 80% of the QDT-calculated f-values agree with NIST values over 20%.

Figure 3 shows a part of the recorded Mg I ablation spectrum that contains one of the solar Mg I lines with narrow emission profiles superposed on broader absorption throughs (Chang & Noyes 1983).

3.3. Revised energy levels

Most of the Ca I and Mg I level energies are already listed in NIST ASD, but some of them were obtained not from laboratory measurements. For instance, 3sng (n = 5–7) and 3s6h levels of Mg I are deduced from solar spectra (Chang 1987), and the same

Table 3. Mg I lines observed in this work.

ν_{ki}, cm^{-1}			Line parameters			Identification
This work	ACE	Biémont & Brault (1986)	I_{ki} (arb. u.)	S/N	$FWHM$, cm^{-1}	
1356.182(2)	1356.152	1356.182 *	1.79×10^4	13.0	0.056(12)	3s5g–3s6h
1406.529(9)	1406.557		3.78×10^3	4.69	0.061(31)	3s5f ^{3}F$_3$–3s6g
2150.348(5)	2150.34	2150.353	4.20×10^2	10.3	0.064(19)	$3s5s\ ^1S_0$–$3s5p\ ^1P_1$
2166.092(17)	2166.08		1.87×10^2	4.09	0.067(41)	3s5g–3s7h
2219.241(13)	2219.31		2.68×10^2	5.90	0.093(38)	3s5f–3s7g
2291.377(8)	2291.463	2291.50	2.13×10^2	6.01	0.068(25)	3s4f^{3}F$_4$–3s5d ^{3}D$_3$
2291.528(27)	2291.55		1.63×10^2	3.70	0.101(89)	3s4f ^{3}F$_3$–3s5d ^{3}D$_2$
2376.286(11)	2376.292	2376.305	2.06×10^2	5.32	0.088(38)	3s5s ^{3}S$_1$–3s5p ^{3}P$_0$
2377.581(5)	2377.579	2377.595	6.06×10^2	11.8	0.092(17)	3s5s ^{3}S$_1$–3s5p ^{3}P$_1$
2380.223(5)	2380.222	2380.236	1.16×10^3	12.8	0.097(15)	3s5s ^{3}S$_1$–3s5p ^{3}P$_2$
2586.006(5)	2586.006	2586.021	6.92×10^5	3.08	0.148(15)	3s4f ^{3}F$_4$–3s5g ^{3}G$_5$
2586.060(1)	2586.047	2586.068	6.51×10^4	2.56	0.031(11)	3s4f ^{3}F$_3$–3s5g ^{3}G$_4$
2586.108(6)	2586.10	2586.110	2.55×10^5	2.13	0.069(23)	3s4f ^{3}F$_2$–3s5g ^{3}G$_3$
2586.326(6)	2586.320	2586.328	1.31×10^5	4.03	0.051(21)	3s4f ^{1}F$_3$–3s5g ^{1}G$_4$
2715.485(3)	2715.502	2715.448	2.28×10^3	19.9	0.116(10)	3s5p ^{3}P$_2$–3s5d ^{3}D$_3$
2718.164(4)	2718.165	2718.119	1.16×10^3	11.1	0.108(14)	3s5p ^{3}P$_1$–3s5d ^{3}D$_2$
2719.450(11)	2719.474	2719.430	2.60×10^2	6.12	0.081(34)	3s5p ^{3}P$_0$–3s5d ^{3}D$_1$
2943.680(5)	2943.694	2943.701	6.44×10^2	15.3	0.094(16)	3s3d ^{1}D$_2$–3s4p ^{1}P$_1$
3011.885(12)	3011.975	3011.893 3011.973	1.89×10^3	3.57	0.173(35)	3s4d ^{3}D$_1$–3s5f ^{3}F$_2$ 3s4d ^{3}D$_2$–3s5f ^{3}F$_3$
3012.046(5)		3012.049	2.88×10^3	6.80	0.144(16)	3s4d ^{3}D$_3$–3s5f ^{3}F$_4$
3209.436(3)	3209.449	3209.447	1.67×10^3	34.2	0.106(9)	3s4p ^{1}P$_1$–3s5s ^{1}S$_0$
4190.106(8)	4190.103	4190.109	3.40×10^4	7.52	0.090(25)	$3s5p\ ^3P_2$–$3s6d\ ^3D_3$
4192.791(17)	4192.785	4192.750	1.35×10^4	4.20	0.093(52)	$3s5p\ ^3P_1$–$3s6d\ ^3D_2$
	4194.069	4194.071				$3s5p\ ^3P_0$–$3s6d\ ^3D_1$
4383.140(6)	4383.144 4383.21	4383.179 4383.225	2.16×10^5	5.38	0.142(18)	3s4d ^{3}D$_1$–3s6f ^{3}F$_2$ 3s4d ^{3}D$_2$–3s6f ^{3}F$_3$
4383.267(4)	4383.28	4383.279	3.08×10^5	7.78	0.142(15)	3s4d ^{3}D$_3$–3s6f ^{3}F$_4$
4746.817(8)		4746.796	5.39×10^4	10.6	0.141(24)	3s4f ^{3}F$_4$–3s7g ^{3}G
4747.101(10)		4747.097	2.09×10^4	6.20	0.086(33)	3s4f ^{1}F$_3$–3s7g ^{1}G$_4$
5843.403(2)		5843.407	2.13×10^6	46.1	0.133(5)	3s4s ^{1}S$_0$–3s4p ^{1}P$_1$
6341.100(3)		6341.095	9.81×10^5	25.5	0.120(8)	3s4p ^{3}P$_2$–3s4d ^{3}D$_3$
6347.891(5)		6347.880	4.85×10^5	12.5	0.115(15)	3s4p ^{3}P$_1$–3s4d ^{3}D$_2$
6351.233(9)		6351.220	1.29×10^5	8.07	0.089(25)	3s4p ^{3}P$_0$–3s4d ^{3}D$_1$
6643.714(5)		6643.712	2.84×10^5	13.8	0.121(14)	3s4s ^{3}S$_1$–3s4p ^{3}P$_0$
6647.013(3)		6647.011	1.12×10^6	14.7	0.142(10)	3s4s ^{3}S$_1$–3s4p ^{3}P$_1$
6653.760(3)		6653.757	2.08×10^6	16.4	0.154(9)	$3s4s\ ^3S_1$–$3s4p\ ^3P_2$
6719.592(4)		6719.596	1.26×10^5	4.58	0.058(12)	3s3d ^{3}D$_1$–3s4f ^{3}F$_2$
6719.714(1)		6719.674 6719.71	2.35×10^5	8.58	0.062(4)	3s3d ^{3}D$_2$–3s4f ^{3}F$_3$ 3s3d ^{3}D$_3$–3s4f ^{3}F$_4$

Notes. (*) Observed by Murcray et al. (1981).

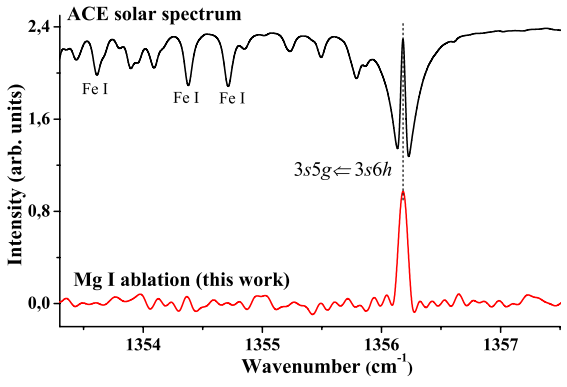

Fig. 3. $5g$–$6h$ Mg I lines from the ablation plasma spectrum (this work) and ACE solar spectrum (Hase et al. 2010).

is the case for 4sng and 4snh ($n = 6, 7$) levels of Ca I (Chang et al. 2000). The energy of the 3s7h level of Mg I is known only from a theoretical estimation (Chang 1987). Table 4 shows the energy values of g and h levels for Mg I and Ca I extracted from the spectra measured in this work.

For Mg I we obtain the energies of g levels using the energies of singlet f levels form Martin & Zalubas (1980) and triplet f levels form Biémont & Brault (1986). In the case of Ca I, we use f level energies from Sugar & Corliss (1985) except for the 4s5g ^{1}G$_4$ level whose energy is calculated from the 3d4p ^{1}F$_3$ level (Sugar & Corliss 1985). The 5g level energies of both atoms are extracted from four lines of the 4f–5g multiplet (see Tables 3, 1). However, the resulting energy values of g levels with different total angular momentum coincide within the uncertainty range (i.e. the fine structure of g levels is not resolved). The exception is the 4s6g ^{3}G$_4$ term in Ca I, which is

Table 4. Values of ng, nh energy levels involved in the observed transitions.

Level	Term	Mg I		Ca I	
		This work	Others	This work	Others
5g	$^1G_4$	57 262.764(8)	57 262.77 [1], 57 262.760 [2]	44 874.416(17)	44 874.149 [3], 44 875.95 [4]
	$^3G_3$	57 262.762(8)		44 874.827(17)	44 874.818 [3], 44 875.96 [4]
	$^3G_4$	57 262.761(5)		44 874.834(21)	44 874.844 [3], 44 875.96 [4]
	$^3G_5$	57 262.761(7)		44 874.858(17)	44 874.875 [3], 44 875.96 [4]
6g	$^1G_4$	58 610.783(10)	58 610.80 [1], 58 610.795 [2]	46 231.672(20)	46 231.7 [3]
	$^3G_3$			46 230.802(23)	46 231.014 [3]
	$3G_4$				46 231.033 [3]
	$^3G_5$			46 231.033(16)	46 231.051 [3]
7g	$^1G_4$	59 423.539(11)	59 423.54 [1], 59 423.537 [2]	47 048.910(16)	47 048.894 [3]
	$^3G_3$	59 423.532(9)		47 048.619(19)	47 048.619 [3]
	$^3G_4$				47 048.636 [3]
	$^3G_5$				47 048.645 [3]
6h	^1H	58 618.944(8)	58 618.942 [2]	46 249.112(19)	46 249.150 [3]
	^3H			46 249.116(21)	
7h	$^{1,3}H$	59 428.854(18)	59 428.853 [2]	47 060.468(24)	47 060.478 [3]

References. [1] Biémont & Brault (1986); [2] NIST (reproduces the data from Chang 1987); [3] Chang et al. (2000); [4] Sugar & Corliss (1985).

clearly resolved. For Mg I, the singlet-triplet separation is also unresolved within the uncertainty. For the h levels, both the fine and the singlet-triplet separation should be even smaller than that for g-levels, and therefore it is also not resolved.

4. Concluding remarks

This work continues a series of FTIR spectroscopy studies of IR spectra of metal atoms (Civiš et al. 2011b,2012b,c) and reports 26 Ca I lines and 3 Mg I lines not observed previously in laboratory measurements. To our knowledge, there are no laboratory-measured spectra of these atoms below 2000 cm^{-1}, therefore this study reports first laboratory observational evidence of some Ca I and Mg I states with high angular momentum (nh and ng states with $n = 6, 7$). A long list of f-values for Ca I and Mg I in the range of 800–9000 cm^{-1} demonstrates good agreement with other experimental and calculated values (when available).

Acknowledgements. This work was financially supported by the Grant Agency of the Czech Republic (grant No. P208/10/2302).

References

Andrievsky, S. M., Spite, M., Korotin, S. A., et al. 2010, A&A, 509, A88
Biémont, E. 1994, in Infrared Solar Physics, eds. D. M. Rabin, J. T. Jefferies, & C. Lindsey, Int. Astron. Union (Dordrecht, Netherlands: Kluwer Academic Publ.), IAU Symp., 154, 501
Biémont, E., & Brault, J. W. 1986, Phys. Scr., 34, 751
Brault, J. W. 1976, J. Opt. Soc. Am., 66, 1081
Brault, J., & Noyes, R. 1983, ApJ, 269, L61
Chang, E. S. 1987, Phys. Scr., 35, 792
Chang, E. S., & Noyes, R. W. 1983, ApJ, 275, L11
Chang, E. S., & Schoenfeld, W. G. 1991, ApJ, 383, 450
Chang, E. S., Avrett, E. H., Noyes, R. W., Loeser, R., & Mauas, P. J. 1991, ApJ, 379, L79
Chang, E., Engleman, R., & Geller, M. 2000, Phys. Essays, 13, 198
Civiš, S., Matulková, I., Cihelka, J., et al. 2010a, Phys. Rev. A, 81, 2510
Civiš, S., Matulková, I., Cihelka, J., et al. 2010b, Phys. Rev. A, 82, 2502
Civiš, S., Kubelík, P., Jelínek, P., Chernov, V. E., & Knyazev, M. Y. 2011a, J. Phys. B, 44, 5006
Civiš, S., Matulková, I., Cihelka, J., et al. 2011b, J. Phys. B, 44, 5002
Civiš, S., Ferus, M., Kubelík, P., Chernov, V. E., & Zanozina, E. M. 2012a, A&A, 545, A61
Civiš, S., Ferus, M., Kubelík, P., Jelinek, P., & Chernov, V. E. 2012b, A&A, 541, A125
Civiš, S., Ferus, M., Kubelík, P., et al. 2012c, A&A, 542, A35
Farmer, C. B., Norton, R. H., & Geller, M. 1989, NASA Ref. Publ., 1224
Glenar, D. A., Reuter, D. C., Deming, D., & Chang, E. S. 1988, ApJ, 335, L35
Hansen, J., Laughlin, C., van der Hart, H., & Verbockhaven, G. 1999, J. Phys. B, 32, 2099
Hase, F., Wallace, L., McLeod, S. D., Harrison, J. J., & Bernath, P. F. 2010, J. Quant. Spectr. Radiat. Transf., 111, 521
Johansson, S. 2005, in High Resolution Infrared Spectroscopy In Astronomy, Proc., ESO Astrophysics Symp., ESO, eds. H. U. Kaufl, R. Siebenmorgen, & A. Moorwood (Berlin, Germany: Springer-Verlag), 62
Kawaguchi, K., Sanechika, N., Nishimura, Y., et al. 2008, Chem. Phys. Lett., 463, 38
Lemoine, B., Petitprez, D., Destombes, J. L., & Chang, E. S. 1990, J. Phys. B, 23, 2217
Martin, W., & Zalubas, R. 1980, J. Phys. Chem. Ref. Data, 9, 1
Mashonkina, L., Korn, A. J., & Przybilla, N. 2007, A&A, 461, 261
Mishenina, T. V., Soubiran, C., Kovtyukh, V. V., & Korotin, S. A. 2004, A&A, 418, 551
Murcray, F. J., Goldman, A., Murcray, F. H., et al. 1981, ApJ, 247, L97
Nilsson, H. 2009, Phys. Scripta, 134, 14009
Pickering, J., Blackwell-Whitehead, R., Thorne, A., Ruffoni, M., & Holmes, C. 2011, Can. J. Phys., 89, 387
Ralchenko, Y., Kramida, A., Reader, J., & NIST ASD Team 2011, NIST Atomic Spectra Database (version 4.1.0)
Risberg, G. 1968, Ark. Fys. (Stockholm), 37, 231
Spite, M., Andrievsky, S. M., Spite, F., et al. 2012, A&A, 541, A143
Sugar, J., & Corliss, C. 1985, J. Phys. Chem. Ref. Data, 14, 1
Sundqvist, J. O., Ryde, N., Harper, G. M., Kruger, A., & Richter, M. J. 2008, A&A, 486, 985
Wahlgren, G. M., van Dishoeck, E. F., Federman, S. R., et al. 2012, Trans. Int. Astron. Union Ser. A, 7, 339
Wallace, L., Livingston, W., Hinkle, K., & Bernath, P. 1996, ApJS, 106, 165
Zhao, G., & Gehren, T. 2000, A&A, 362, 1077
Zhao, G., Butler, K., & Gehren, T. 1998, A&A, 333, 219